Published in *Fluctuations and Noise in Photonics and Quantum Optics II*, eds. P. Heszler, D. Abbott, J.R. Gea-Banacloche and P. R. Hemmer, Proc. of SPIE vol. 5468, Bellingham, 2004, pp 133-141.

Polarisation Switches in Vertical Cavity Surface Emitting Lasers

Stefano Beri[a], Riccardo Mannella[b], Dmitri G. Luchinsky[a], Peter V. E. McClintock[a]

[a]Department of Physics, Lancaster University LA1 4YB, Lancaster, United Kingdom;
[b]Dipartimento di Fisica, Università di Pisa Via Buonarroti 2, Pisa, Italy.

ABSTRACT

The polarization dynamics of a vertical cavity surface emitting laser is investigated as a nonlinear stochastic dynamical system. The polarization switches in the device are considered as activation processes in a two dimensional system with a saddle cycle; the optimal way of switching is determined as the solution of a boundary value problem. The theoretical results are in good agreement with the numerical simulations.

Keywords: Vertical cavity surface emitting lasers, Polarization dynamics, Activation problems.

1. INTRODUCTION

Vertical Cavity Surface Emitting Lasers (VCSEL) are a novel class of semiconductor lasers which are having great success in many applications requiring high speed, precision and efficiency. VCSELs promise to revolutionize fibre optic communications by improving efficiency and increasing data speed. Nowadays VCSELs allow computer networks transmit reliably data at rates of up to and beyond 10Gb/s. Other successful applications of VCSEL are in the realization of proximity sensors, encoders, laser range finders, laser printing, bar code scanning, optical storage.

Among the many benefits of VCSEL compared to over edge-emitting diodes, VCSELs are cheaper to manufacture in quantity, they are easier to test, and they are more efficient. Moreover, the VCSELs require less electrical current to produce a given coherent energy output. VCSELs emit a narrow, more nearly circular beam than traditional edge emitters; this makes it easier to get the energy from the device into an optical fiber. It is expected that in the nearest future, VCSEL will be one of the most popular laser diodes for the majority of the applications.

The main feature in VCSEL design is the cylindrical symmetry of the active cavity: this allows one to fabricate two dimensional arrays of lasers and reduces dramatically the astigmatism of the beam. Unfortunately the applicability of VCSEL is limited by the presence of different instabilities in the polarization dynamics. Consider for example a VCSEL emitting in the fundamental transverse mode; due to the circular design of the active medium, no well defined directions for the polarization are expected. Nevertheless, there is experimental evidence that, for the majority of the cases, the VCSEL emission just above threshold is with a well defined linear polarization.[1] Increasing the pumping current, the direction of the polarization changes from the first mode to the orthogonal one.[2] For intermediate pumping current, both linear polarized states are stable, and the VCSEL is observed to perform spontaneous transitions between the two modes.[3] For very high values of the pumping current, both modes lose their stability[4–6] and higher order transverse modes appear. We stress that all these features are intrinsic in the VCSEL due to the geometry of the device and that they have to be properly understood in order to move toward a generation of VCSELs that are more efficient and reliable.

Different attempts to control the polarization emission have been done by breaking in a controlled way the symmetry of the device, for example with non-symmetrical growth of the active medium, or using "local burning"[7] or "hot spot" techniques.[8] A different approach to the polarization control have been attempted using optical injection in a master-slave configuration[9] or optical feedback.[10]
From a theoretical point of view, a big effort has been made in order to understand how the presence of

Further author information: send correspondence to Stefano Beri: s.beri@lancaster.ac.uk or to Riccardo Mannella: mannella@df.unipi.it

anisotropies in the mirrors and cavity,[4] axial magnetic field, and polarization dependent saturation affects the polarization of the emitted light.
A very promising model that allows a full nonlinear description of the VCSEL emission was introduced in 1995 by San Miguel, Feng and Moloney (SFM).[11] Although clear and realistic, the SFM model is still too complicated to allow a simple solution; many different ways have been been attempted to decouple the polarization dynamics from that of the internal medium, including the use of normalized Stokes components[12] and polarization angles.[6] In this last approach, the dynamics of the angles is described by a set of two nonlinear coupled differential equations and the spontaneous emission of photons is described by introducing two stochastic terms. In the bistability regime, the system presents two stable points corresponding to the two polarization modes whose basins of attraction are separated by an unstable limit cycle. The presence of spontaneous emission allows the system to move away from the stable states and explore different states of polarization. When the noise intensity is small, the system spends the majority of the time in the vicinity of one of the stable states, but, occasionally, an exceptional noise burst can drive the system to the basin of attraction of the other polarization state and a polarization transition is observed.
The small fluctuations in the vicinity of the steady states have been carefully investigated in the linear regime.[6,13–15] However, the investigation of the large fluctuations (involving a full nonlinear treatment) and, in particular, of the polarization switches in the devices is far from being completed.
A possible way to approach the problem comes from the study of *activation problems* in stochastic nonlinear systems.[16] The main result achieved is that, in the limit of zero noise intensity, the polarization switch is expected to take place in a ballistic manner along a most probable transition path (MPTP) that can be obtained from an auxiliary Hamiltonian system.[17–24]
In this paper we consider a VCSEL emitting in the fundamental transverse mode in the bistable polarization regime. The dynamics of the polarization is described using the polarization angles.[6] Polarization switches are investigated in the regime of small noise intensity. The MPTP and the activation energy are found for different values of the pumping parameters.

2. THEORY

2.1 VCSEL emission

In this section we summarize the theory for the polarization dynamics of the VCSEL. The SFM model[11] approximates the band structure of the active medium as a two-level system. The upper level (conduction band) is populated by electrons having total angular momentum $J = \frac{1}{2}$* and projection in the axis direction $J_z = \pm\frac{1}{2}$. The lower level (heavy holes band) is populated by electrons having total angular momentum $J = \frac{3}{2}$ and projected angular momentum $J_z = \pm\frac{3}{2}$.
In the dipole approximation two independent electronic transitions are involved: $+\frac{3}{2} \longrightarrow +\frac{1}{2}$ (and the inverse) and $-\frac{3}{2} \longrightarrow -\frac{1}{2}$ (and its inverse). Due to the conservation of angular momentum, two separate classes of circular polarized photons are involved in the two transitions. The two families of electrons are coupled by a large number of different relaxation processes,[11] for example interaction with static scatterers[25] or electron-hole exchange interaction.[26] All these processes are summarized in the SFM model introducing a phenomenological *spin-flip* rate. The two families of photons are directly coupled by the presence of amplitude and phase anisotropies in the cavity or in the mirrors.[4] Including all these effects, the following rate equations[11] for the emission of the VCSEL are obtained

$$\begin{aligned}
\dot{E}_{\pm} &= -\left(\gamma_l + i\omega_l\right) E_{\mp} + k\left(1 - i\alpha\right)\left(D \pm d - 1\right) E_{\pm} \\
\dot{D} &= -\gamma_{||} D + \gamma_{||}\left(\Lambda + 1\right) - \gamma_{||}\left[\left(|E_+|^2 + |E_-|^2\right) D - \left(|E_+|^2 - |E_-|^2\right) d\right] \\
\dot{d} &= -\gamma_J d - \left[\left(|E_+|^2 - |E_-|^2\right) D - \left(|E_+|^2 + |E_-|^2\right) d\right]
\end{aligned} \quad . \tag{1}$$

Here $E_{\pm}$ represent the slowly-varying components of the clockwise and anti-clockwise electric fields; D is the average insertion population of the two families of electrons and d indicates half the difference in the inversion population. Different parameters are present in the model, describing the effect of anisotropies and dissipation processes in the active media (and in the mirrors): γ_l and ω_l are the absorptive and dispersive linear anisotropies;

*All angular momenta are given in units of $\hbar$

$\gamma_{||}$ is the decay rate of the inversion population and γ_J is the spin-flip rate measuring how often electrons spontaneously move from one family to the other. Λ is the dimensionless pumping factor normalized at the threshold, α is the linewidth enhancement factor and κ is the average lifetime of a photon in the cavity. The dimensionless parameter $\Gamma = \frac{\gamma_J}{\gamma_{||}}$ measures the relative importance of the spin-flip and the relaxation. A small value of Γ indicates that the electrons behave mainly as two separate families and the coupling between the two polarization mode take place mainly through anisotropies. On the other hand, a large value of Γ indicates that the electrons behave as a single reservoir for the two circular polarized modes and the two modes are strongly coupled even with very small anisotropies. It is an experimental result that typical values of Γ for a standard VCSEL exceed 100.
The stationary polarization modes of the VCSEL can be obtained from (1) introducing a trial-solution of the form

$$\begin{aligned} E_+ &= \pm E_- = A \exp\left[-i\omega t\right] && (2)\\ D &= D_0 && (3)\\ d &= 0. && (4) \end{aligned}$$

The mode with $E_+ = \pm E_-$ corresponds to $\hat{x}$-polarized light, while $E_+ = -\pm E_-$ correspond to $\hat{y}$-polarized light. Substituting (2-4) in (1), the following relations are obtained

$$\begin{aligned} A &= \sqrt{\frac{1}{2}\frac{\Lambda \mp \frac{\gamma_l}{\kappa}}{1 \pm \frac{\gamma_l}{\kappa}}} && (5)\\ D_0 &= 1 \pm \frac{\gamma_l}{\kappa} && (6)\\ \omega &= \pm\omega_l \pm \alpha\gamma_l && (7) \end{aligned}$$

It is clear that the two linearly polarized modes have slightly different frequencies; therefore, intensities and gains differ slightly in the two modes. In particular, it is possible that for small pumping currents, only one of the modes is steadily lasing. In what follows, we consider the pumping to be big enough to allow lasing in both modes.

Outside the linear regime, the set of equations (1) is very complicated and it requires further simplification in order to achieve an understanding of the polarization dynamics. It is a well known result that the polarization of the radiation can be described as a flow on the unitary sphere in the space of the normalized Stokes component s_i where

$$\begin{cases} s_1 = \cos(2\chi)\cos(2\phi) = 2\frac{\Re\left[E_+^* E_-\right]}{I} \\ s_2 = \cos(2\chi)\sin(2\phi) = 2\frac{\Im\left[E_+^* E_-\right]}{I} \\ s_3 = \sin(2\chi) = \frac{|E_+|^2 - |E_-|^2}{I} \\ I = |E_+|^2 + |E_-|^2 \end{cases} \quad (8)$$

Here I represents the intensity of the radiation, and the two angles χ and ϕ represent the ellipticity and the direction of the polarization respectively. The two linearly polarized stable solutions of (1) corresponds to $s_1 = \pm 1$, $s_2 = s_3 = 0$. The differential equations satisfied by the angles χ and ϕ can be obtained by substitution of (8) into the rate equations (1). As a result, the following system is obtained

$$\begin{aligned} \dot{\chi} &= \omega_l \sin(2\phi) - 2\kappa\gamma d \sin(2\chi)\cos(2\chi) + \gamma_l \sin(2\chi)\cos(2\phi). && (9)\\ \dot{\phi} &= -\omega_l \frac{\sin(2\chi)}{\cos(2\chi)}\cos(2\phi) - \gamma_l \frac{\sin(2\phi)}{\cos(2\chi)} + 2\alpha\kappa d. && (10)\\ \dot{I} &= -2\gamma_l I \cos(2\chi)\cos(2\phi) + 2\kappa\left(D-1\right)I + 2\kappa d I \sin(2\chi) && (11)\\ \dot{D} &= -\gamma_{||} D + \gamma_{||}\left(\Lambda + 1\right) - \gamma_{||}\left[ID - I\sin(2\chi)d\right] && (12)\\ \dot{d} &= -\gamma_J d - \left[I\sin(2\chi)D - Id\right] && (13) \end{aligned}$$

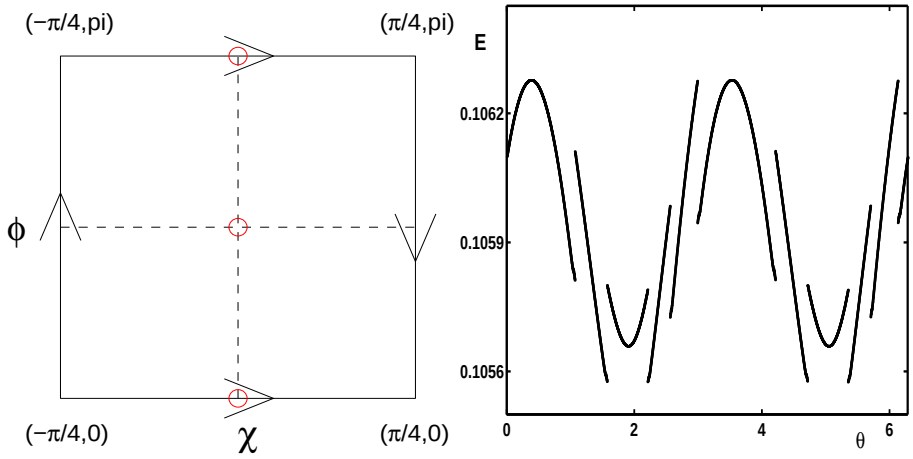

Figure 1. (Left) The topology of the space of the angles. The sides of the square have to be identified according to the arrows. In particular, $\phi = 0$ and $\phi = \pi$ are identified as a cylinder, whilst $\chi = -\pi/4$ and $\chi = \pi/4$ are identified as a Moebius Stripe. The result of this is a Klein Bottle. The states with $\chi = 0$ are the linearly polarized states. The polarization angle ϕ defines the the direction of the linear polarization.The circles indicate the stationary solution of Eq.(15) and (16). (Right) The "Escape Energy" for the escape problem as a function of the parameter θ. The global minimum of the action corresponds to the MPTP.

The dynamics of the polarization couples with the dynamics of the intensity and the internal dynamics of the medium through the average difference in the inversion population. Introducing some approximations, the dynamics of the angles can be fully decoupled from the other dynamical variables. In the limit of large values of Γ, the dynamics of d can be adiabaticaally eliminated to give

$$d = -\frac{I}{\Gamma} s_3 = -\frac{I}{\Gamma} \sin(2\chi). \tag{14}$$

Moreover, for small values of pumping and dichroism, the intensity of the radiation can be considered to be constant. Introducing these approximations, the final result for the dynamics of the angles χ and ϕ is obtained:

$$\dot{\chi} = f_\chi(\chi,\phi) = \omega_l \sin(2\phi) - \frac{2\kappa\Lambda}{\Gamma}\sin(2\chi)\cos(2\chi) + \gamma_l \sin(2\chi)\cos(2\phi); \tag{15}$$

$$\dot{\phi} = f_\phi(\chi,\phi) = -\omega_l \frac{\sin(2\chi)}{\cos(2\chi)}\cos(2\phi) + \gamma_l \frac{\sin(2\phi)}{\cos(2\chi)} - \frac{2\alpha\kappa\Lambda}{\Gamma}\sin(2\chi). \tag{16}$$

where the effects of radiation intensity are included in the so-called non-linear anisotropies: $\gamma_n = 2\frac{\kappa\Lambda}{\Gamma}$ and $\omega_n = \alpha\gamma_n$. They are the nonlinear absorptive anisotrpy and nonlinear dispersive anisotropy. It is clear that they depend explicitly on the pumping parameter Λ i.e. on the number of photons present in the active medium.
Eq. (15) and (16) completely describe the dynamics of the polarization of the VCSEL emission. Their solution is a smooth flow on the angle space $-\pi/4 < \chi < \pi/4$ and $0 < \phi < \pi$ which is diffeomorph to a Klein Bottle as shown in figure 1. The flows admit two stationary points $\chi = 0; \phi = \pi/2$ and $\chi = 0; \phi = 0 \equiv \pi$ corresponding to $\hat{y}$-polarized and $\hat{x}$-polarized linear modes. The stability of the two modes is obtained by linearisation of Eq.(15) and (16) about the stable points.[6] The stability of the modes depends on the interplay of linear and nonlinear anisotropies; for a device with small enough dicrohism, both modes are stable even for small values of the pumping parameter Λ. In this *bistability* regime, the basins of attractions of the two modes are separated by a saddle cycle. The shape of the cycle is determined by the interplay of all the anisotropies in the system.

2.2 The fluctuations: solution of the boundary value problem

The system of equations (15) and (16) is purely deterministic. In order to describe a real device satisfactorily, the spontaneous emission has to be taken into account. In this talk, we describe the spontaneous emission of

photons in the laser cavity phenomenologically: two stochastic terms ξ_χ and ξ_ϕ are introduced in Eq.(15) and (16). The full system describing the polarization dynamics including noise is

$$\begin{aligned}
\dot{\chi} &= f_\chi(\chi,\phi) + \xi_\chi(t) && (17)\\
\dot{\phi} &= f_\phi(\chi,\phi) + \xi_\phi(t) && (18)\\
\langle \xi_\chi(t) \rangle &= \langle \xi_\phi(t) \rangle = 0 \quad \forall t && (19)\\
\langle \xi_\chi(t)\xi_\chi(s) \rangle &= \langle \xi_\phi(t)\xi_\phi(s) \rangle = \epsilon\delta(t-s) \quad \langle \xi_\phi(t)\xi_\chi(s) \rangle = 0 \quad \forall t,s && (20)
\end{aligned}$$

here $f_\chi(\chi,\phi)$ and $f_\phi(\chi,\phi)$ are the drift field introduced in Eq.(15) and (16); $\xi_\chi(t)$ and $\xi_\phi(t)$ are two uncorrelated Gaussian processes with intensity ϵ describing the spontaneous emission in the system. Due to the presence of the noise, the system has a certain non-zero probability of exploring regions of the angle-space (i.e. polarization states) different than the stable ones. The probability distribution $\rho(\chi,\phi,t)$ for (17) and (18) satisfies the Fokker-Planck equation

$$\frac{\partial \rho}{\partial t} = -\frac{\partial f_\chi \rho}{\partial \chi} - \frac{\partial f_\phi \rho}{\partial \phi} + \frac{\epsilon}{2}\left(\frac{\partial^2 \rho}{\partial \chi^2} + \frac{\partial^2 \rho}{\partial \chi^2}\right) \tag{21}$$

In the limit of small noise intensity, (21) can be solved to different orders using the WKB approximation.[17,19,21–23,27–31] Introducing a trial-function of the form

$$\rho = Z e^{-\frac{S}{\epsilon}} \tag{22}$$

in (21), and considering the leading order ϵ^{-1}, the following Hamilton-Jacobi equation for the potential $S(\chi,\phi,t)$ is obtained

$$\frac{\partial S}{\partial t} + H\left(\frac{\partial S}{\partial \chi}, \frac{\partial S}{\partial \phi}, \chi, \phi\right) = 0 \tag{23}$$

where $H\left(p_\chi, p_\phi, \chi, \phi\right) = \frac{p_\chi^2 + p_\phi^2}{2} + p_\chi f_\chi + p_\phi f_\phi$ and $p = \nabla f$. The Hamilton equations associated with (23) are

$$\begin{aligned}
\dot{\chi} &= \frac{\partial H}{\partial p_\chi} = f_\chi + p_\chi && (24)\\
\dot{\phi} &= \frac{\partial H}{\partial p_\phi} = f_\phi + p_\phi && (25)\\
\dot{p}_\chi &= -\frac{\partial H}{\partial \chi} = -\frac{\partial f_\chi}{\partial \chi} p_\chi - \frac{\partial f_\phi}{\partial \chi} p_\phi && (26)\\
\dot{p}_\phi &= -\frac{\partial H}{\partial \phi} = -\frac{\partial f_\chi}{\partial \phi} p_\chi - \frac{\partial f_\phi}{\partial \phi} p_\phi && (27)
\end{aligned}$$

and the potential S evolves along the trajectories according to

$$\dot{S} = \frac{1}{2}\left(p_\chi^2 + p_\phi^2\right) \tag{28}$$

According to (22), in the limit of $\epsilon \to 0$, the probability of observing a polarization transition can be expressed by calculation of the potential S along a trajectory solution of (24-27) that leave the initial stable state and reaches the saddle cycle. It is well known[27,32–34] that there are many solutions of (24-27) that emanate from the initial state and reach the limit cycle, each of them with a different value of S. According to (22), when $\epsilon \to 0$, only the trajectory with the least S contributes to the transition; all other trajectories are exponentially disadvantaged. The trajectory that minimizes S is the MPTP.
It is well known[22,35] that the MPTP is an heteroclinic trajectory leaving the initial steady polarization state for $t \to -\infty$ and reaching the saddle cycle asymptotically for $t \to \infty$. From the topological point of view, the trajectories emanating from the initial state $t \to -\infty$ form its unstable Lagrangian manifold M^u; in the same way, the trajectories converging to the saddle cycle for $t \to \infty$ form its stable manifold M^s. The MPTP lies on the intersections of the two manifolds.

The key step to find the MPTP among all other trajectories emanating from the initial state is a proper characterization of the Lagrangian manifold in the vicinity of the initial state. In a small neighborhood of the

initial state, the unstable manifold is a plane in the phase space. The equations describing the shape of M^u can be obtained by linearisation of the Hamiltonian equations (24-27) around the stationary point

$$\frac{d}{dt}\begin{pmatrix}\delta\chi\\ \delta\phi\\ p_\chi\\ p_\phi\end{pmatrix}=\begin{pmatrix}\frac{\partial f_\chi}{\partial\chi} & \frac{\partial f_\chi}{\partial\phi} & 1 & 0\\ \frac{\partial f_\phi}{\partial\chi} & \frac{\partial f_\phi}{\partial\phi} & 0 & 1\\ 0 & 0 & -\frac{\partial f_\chi}{\partial\chi} & -\frac{\partial f_\phi}{\partial\chi}\\ 0 & 0 & -\frac{\partial f_\chi}{\partial\phi} & -\frac{\partial f_\phi}{\partial\phi}\end{pmatrix}\begin{pmatrix}\delta\chi\\ \delta\phi\\ p_\chi\\ p_\phi\end{pmatrix}. \tag{29}$$

where $\delta\chi$ and $\delta\phi$ represent the displacements from the stationary states and the partial derivatives are evaluated in the steady states. The unstable manifold is spanned by the two expanding eigenvalues $\vec{v}_1^u$ and $\vec{v}_2^u$ of the system. A generic point on M^u can be written as $\vec{v}=\alpha_1\vec{v}_1^u+\alpha_2\vec{v}_2^u$ where $\alpha_{1,2}$ are complex coefficients.
Separating the angles and the momenta, the following relations are obtained

$$\begin{pmatrix}\delta\chi\\ \delta\phi\end{pmatrix} = \begin{pmatrix}v_{1\chi} & v_{2\chi}\\ v_{1\phi} & v_{2\phi}\end{pmatrix}\begin{pmatrix}\alpha_1\\ \alpha_2\end{pmatrix}$$
$$\begin{pmatrix}p_\chi\\ p_\chi\end{pmatrix} = \begin{pmatrix}v_{1p_\chi} & v_{2p_\chi}\\ v_{1p_\phi} & v_{2p_\phi}\end{pmatrix}\begin{pmatrix}\alpha_1\\ \alpha_2\end{pmatrix}$$

Using standard linear algebra techniques, the linear relation between x and p is obtained in the form $p=Mx$ where the matrix M is defined as

$$M=\begin{pmatrix}v_{1p_\chi} & v_{2p_\chi}\\ v_{1p_\phi} & v_{2p_\phi}\end{pmatrix}\begin{pmatrix}v_{1\chi} & v_{2\chi}\\ v_{1\phi} & v_{2\phi}\end{pmatrix}^{-1}. \tag{30}$$

Because the relationship between coordinates and momenta is known (the matrix M in Eq.(30)), it is enough to provide a characterization of the trajectories in the coordinate space.
For a two-dimensional continuous system such as (15-16), the trajectories emanating from the initial stable point are a one-parameter family on the phase space. A possible choice for the parameterisation in the vicinity of a stable point can be the following: consider a small circle of given radius r around the stable point (r should be small enough for the application of Eq.(30)). The initial conditions for the trajectories are taken on this circle and the corresponding initial momenta are calculated using (30). In this way the unstable manifold is completely parameterised. From the topological point of view, the parameters space is diffeomorph to a circle S^1.
The activation energy can now be calculated as a function of the initial conditions (i. e. of the parameter θ) $S:S^1\longrightarrow R$.
According to the discussion above, the minimum of the function S in the parameter space corresponds to the initial conditions defining the MPTP.

3. POLARIZATION TRANSITIONS

The activation energy as a function of the parameters can be plotted as an *action plot*, as in figure 1(right). The main feature of the graph is the presence of many discontinuities corresponding to local minima. The presence of degenerate minima are a consequence of the central symmetry in the set (24-27): for every possible value of the noise intensity, the polarization transition occurs with the same probability along two centrally symmetrical paths. The absolute minimum of the action corresponds to the MPTP.

In order to show the agreement of the theory, in figure 2 (left) the MPTP calculated using the minimisation technique is plotted together with a numerical solution of (17-18). Close agreement between them is evident. It should be noted that, in the vicinity of the saddle cycle, the numerical trajectory diverges from the theory due to finite noise diffusion. This effect can be included in the theory expanding the Fokker-Planck equation (21) at the next-to-the-leading order in order to include finite noise contributions.[36]
We now consider a typical VCSEL, and we vary the pumping current. According to the equations (15-16), this induces a change in the nonlinear anisotropies, while the linear anisotropies are left unchanged. We consider a standard device having birefringence ω_l as its dominant anisotropy and we calculate the activation energy for different values of γ_n (i.e. different values of the pumping rate Λ). The activation energy is plotted for different

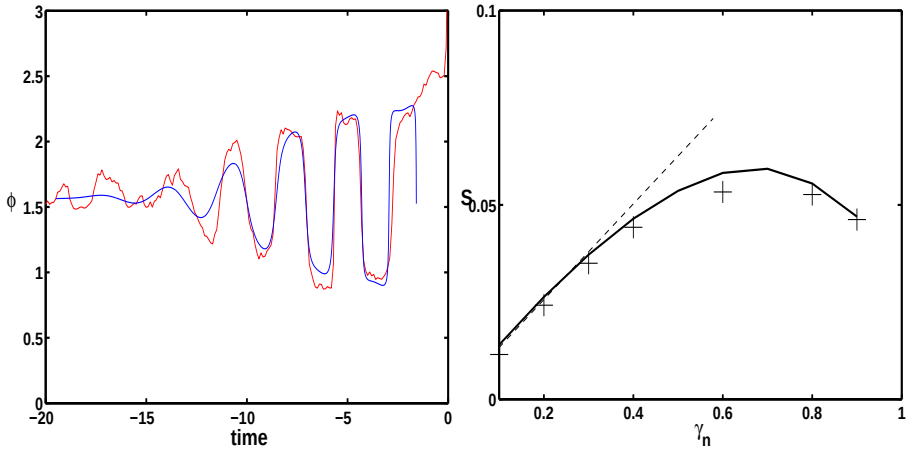

Figure 2. (Left) Comparison between theoretical MPTP and a realization of the transition calculated via numerical simulation. The agreement between the two paths is excellent. The divergence of the experiment from the theory is due to finite noise diffusion.(Right) The dependence of the activation energy on the nonlinear dichrohism. The maximum of the activation energy corresponds to an exponentially stable polarization. The crosses are the results of numerical simulations. For small values of γ_n there is an almost linear dependence of S on the pumping parameter.

values of γ_n in figure 2 (right). The main feature of the activation energy is its non-monotony: for small above threshold values of γ_n, the stability of the mode increases with pumping; but for higher pumping rates, the dependence inverts and the injection of more current into the system reduces the polarization stability.
The dashed line in figure 2 (right) represents the regime where the dynamics of the two fast-rotating Stokes components s_2 and s_3 can be averaged out reducing the system to a double-well potential. The actual activation energy is then smaller than that calculated using the simplified double-well model. From the physical point of view, the behavior of the activation energy can be justified as follow. When the system is close to the threshold and the nonlinear anisotropies can be neglected, an increase in the pumping current means an increase of the photons in the lasing mode according to Eq.(5) To induce a polarization switch in this regime, a fluctuation should suddenly damp the photons in one mode and at the same time produce photons in the other. It is clear that such an event is disadvantaged by the presence of many photons in the lasing mode. On the other hand, when the pumping current is big enough, it starts affecting the stability of the lasing mode. In this regime an increase of the pumping reduce the stability of the modes and the fluctuation are strongly amplified. As a consequence, the activation energy is reduced by an increase in the pumping because the stability of the mode decreases. This particular shape of the activation energy suggests that the driving current can be used to control the stability of the polarization modes and eventually favorite the stability of one of the modes on the others.

4. SUMMARY AND CONCLUSIONS

In this talk, we investigated the full nonlinear polarization dynamics of a VCSEL emitting in the fundamental transverse mode. The system of Maxwell-Bloch equations for the laser emission is reduced to a two-dimensional system describing the polarization state of the device. The presence of spontaneous emission in the system has been treated introducing stochastic terms into the polarization dynamics. In the limit of small noise intensity, the stochastic dynamics of the polarization has been mapped to a four-dimensional Hamiltonian problem, and the calculation of the activation energy for a polarization switch has been obtained by minimisation of the cost function along Hamiltonian trajectories. In order to perform the minimisation properly, the unstable Lagrangian manifold of the steady polarization modes has been calculated using linear expansion, and the family of Hamiltonian trajectories has been conveniently parameterised with one parameter θ. Taking the minimum of the energy as a function of θ, the most probable transition path has been located. It is in a good agreement with the results of simulations for different values of the system's parameters.
The activation energy dependence on the nonlinear dichroism (i.e. pumping parameter) has been shown to be nonmonotonic. In particular, the presence of a maximum in the activation energy suggests that the linear polarized modes can be made exponentially more stable choosing a proper value of the external pumping.

REFERENCES

1. J. L. Jewell, S. L. McCall, Y. H. Lee, A. Scherer, A. C. Gossard, and J. H. English, "Lasing characteristic of gaas microresonators," *Appl. Phys. Lett.* **54**, pp. 1400–1402, 1989.
2. C. J. Chang-Hasnain, J. P. Harbison, L. T. Florez, and N. G. Stoffel, "Polarization characteristics of quantum-well vertical cavity surface emitting lasers," *Electron. Lett.* **27**, pp. 163–165, 1991.
3. K. D. Choquette, R. S. Jr., K. L. Lear, and R. E. Leibenguth, "Gain-dependent polarization properties of vertical-cavity lasers," *IEEE J. Sel. Top. Quantum Electron.* **1**, pp. 661–666, 1995.
4. M. Travagnin, M. van Exter, A. K. J. van Doorn, and J. P. Woerdman, "Role of optical anisotropies in the polarization properties of surface-emitting semiconductor lasers," *Phys. Rev. A* **54**, pp. 1647–1660, 1996.
5. J. Martin-Regalado, F. Prati, M. S. Miguel, and N. B. Abraham, "Polarization properties of vertical-cavity surface-emitting lasers," *IEEE J. Quantum Electron.* **33**, pp. 765–783, 1997.
6. M. P. van Exter, R. F. M. Hendriks, and J. P. Woerdman, "Physical insight into the polarization dynamics of semiconductor vertical-cavity lasers," *Phys. Rev. A* **57**, pp. 2080–2090, 1998.
7. A. K. J. van Doorn, M. van Exter, and J. P. Woerdman, "Tailoring the birefringence in a vertical-cavity semiconductor laser," *Appl. Phys. Lett.* **69**, pp. 3635–3637, 1996.
8. A. K. J. van Doorn, M. van Exter, and J. P. Woerdman, "Elasto-optic anisotropy and polarization orientation of vertical-cavity surface-emitting semiconductor lasers," *Appl. Phys. Lett.* **69**, pp. 1041–1043, 1996.
9. S. Banyopadhyay, Y. Hong, P. Spencer, and K. A. Shore, "VCSEL polarization control by optical injection," *J. Lighwave Technol.* **21**, 2003.
10. S. Sivaprakasam, S. Banyopadhyay, Y. Hong, P. Spencer, and K. A. Shore, "Polarization-resolved relative intensity noise measurements of a vertical-cavity surface-emitting laser subject to strong optical feedback," *IEEE Photon. Techno. Lett.* , in press.
11. M. S. Miguel, Q. Feng, and J. V. Moloney, "Light-polarization dynamics in surface-emitting semiconductor lasers," *Phys. Rev. A* **52**, pp. 1728–1739, 1995.
12. M. B. Willemsen, M. P. van Exter, and J. Woerdman, "Anatomy of a polarization switch of a vertical-cavity semiconductor laser," *Phys. Rev. Lett* **84**, pp. 4337–4340, 2000.
13. M. B. Willemsen, M. P. van Exter, and J. P. Woerdman, "Correlated fluctuations in the polarization modes of a vertical cavity semiconductor laser," *Phys. Rev. A* **60**, pp. 4105–4113, 1999.
14. M. P. van Exter, M. B. Willemsen, and J. P. Woerdman, "Polarization fluctuations in vertical-cavity semiconductor lasers," *Phys. Rev. A* **58**, pp. 4191–4205, 1998.
15. H. F. Hofmann and O. Hess, "Polarization fluctuations in vertical-cavity surface-emitting lasers: a key to the mechanism behind polarization stability," *Quantm Semiclass. Opt.* **10**, pp. 87–96, 1998.
16. V. I. Mel'nikov, "The kramers problem: fifty years of development," *Phys. Rep.* **209**, pp. 1–71, 1991.
17. D. Ludwig, "Persistence of dynamical systems under random perturbations," *SIAM Rev.* **17**, pp. 605–640, 1975.
18. M. Freidlin and A. D. Wentzel, *Random Perturbations in Dynamical Systems*, Springer, New York, 1984.
19. R. S. Maier and D. L. Stein, "Effect of focusing and caustics on exit phenomena in systems lacking detailed balance," *Phys. Rev. Lett.* **71**, pp. 1783–1786, 1993.
20. R. S. Maier and D. L. Stein, "How an anomalous cusp bifurcates in a weak-noise system," *Phys. Rev. Lett.* **85**, pp. 1358–1361, 2000.
21. M. I. Dykman, M. M. Millonas, and V. N. Smelyanskiy, "Observable and hidden features of large fluctuations in nonequilibrium systems," *Phys. Lett. A* **195**, pp. 53–58, 1994.
22. V. N. Smelyanskiy and M. I. Dykman, "Topological features of large fluctuations to the interior of a limit cycle," *Phys. Rev. E* **55**, p. 2516, 1997.
23. R. S. Maier and D. L. Stein, "A scaling theory of bifurcations in the symmetrical weak-noise escape problem," *J. Stat. Phys.* **83**, pp. 291–357, 1996.
24. J. Lehmann, P. Reimann, and P. Hanggi, "Surmounting oscillating barriers: path-integral approach for weak noise," *Phys. Rev. E* **62**, pp. 1639–1642, 2000.
25. R. Ferreira and G. Bastard, ""Spin"-flip scattering of holes in semiconductor quantum wells," *Phys. Rev B* **43**, pp. 9687–9691, 1991.

26. M. Z. Maialle, E. A. de Andreada e Silva, J. Shah, and L. J. Sham, "Exciton spin dynamics in quantum wells," *Phys. Rev. B* **47**, pp. 15776–15788, 1993.
27. M. V. Day, "Recent progress on the small parameter exit problem," *Stochastics* **20**, pp. 121–150, 1987.
28. A. J. McKane, "Noise-induced escape rate over a potential barrier: Results for a general noise," *Phys. Rev. A* **40**(7), pp. 4050–4053, 1989.
29. M. I. Dykman, "Large fluctuations and fluctuational transitions in systems driven by colored gaussian noise–a high frequency noise," *Phys. Rev. A* **42**, pp. 2020–2029, 1990.
30. S. J. B. Einchcomb and A. J. McKane, "Escape rates in bistable systems induced by quasi-monochromatic noise," *Phys. Rev. E* **49**, pp. 259–266, 1994.
31. R. S. Maier and D. L. Stein, "Oscillatory behaviour of the rate of escape through an unstable limit-cycle," *Phys. Rev. Lett.* **77**, pp. 4860–4863, 1996.
32. V. Arnold, *Mathematical Methods of Classical Mechanics*, Springer-Verlag, Berlin, 1978.
33. R. Graham and T. Tel, "Existence of a potential for dissipative dynamical systems," *Phys. Rev. Lett.* **52**, pp. 9–12, 1984.
34. H. R. Jauslin, "Nondifferentiable potentials for nonequilibriumsteady states," *Physica A* **144**, pp. 179–191, 1987.
35. R. S. Maier and D. L. Stein, "Limiting exit location distributions in the stochastic exit problem," *SIAM J. Appl. Math.* **57**, pp. 752–790, 1997.
36. A. Bandrivskyy, S. Beri, and D. G. Luchinsky, "Noise-induced shift of singularities in the pattern of optimal paths," *Phys. Lett. A* **314**, pp. 386–391, 2003.